



# Observations of the thermodynamic and kinematic state of the atmospheric boundary layer over the San Luis Valley, CO using remotely piloted aircraft systems during the LAPSE-RATE field campaign

Elizabeth A. Pillar-Little<sup>1,2</sup>, Brian R. Greene<sup>1,2,3</sup>, Francesca M. Lappin<sup>1,2</sup>, Tyler M. Bell<sup>1,2,4,5</sup>, Antonio R. Segales<sup>2,3,6</sup>, Gustavo Britto Hupsel de Azevedo<sup>2,6</sup>, William Doyle<sup>2</sup>, Sai Teja Kanneganti<sup>2,7</sup>, Daniel D. Tripp<sup>4,5</sup>, and Phillip B. Chilson<sup>1,2,3</sup>

<sup>1</sup>School of Meteorology, University of Oklahoma, Norman, OK 73072, USA

<sup>2</sup>Center for Autonomous Sensing and Sampling, University of Oklahoma, Norman, OK 73072, USA

<sup>3</sup>Advanced Radar Research Center, University of Oklahoma, Norman, OK 73019, USA

<sup>4</sup>Cooperative Institute for Mesoscale Meteorological Studies, University of Oklahoma, Norman, OK 73072, USA

<sup>5</sup>NOAA/OAR National Severe Storms Laboratory, Norman, OK 73072, USA

<sup>6</sup>School of Electrical and Computer Engineering, University of Oklahoma, Norman, OK 73019, USA

<sup>7</sup>School of Computer Science, University of Oklahoma, Norman, OK 73019, USA

**Correspondence:** Elizabeth A. Pillar-Little (epillarlittle@ou.edu)

**Abstract.** In July 2018, the University of Oklahoma deployed three CopterSonde 2 remotely piloted aircraft systems (RPAS) to take measurements of the evolving thermodynamic and kinematic state of the atmospheric boundary layer (ABL) over complex terrain in the San Luis Valley, Colorado. A total of 180 flights were completed over five days, with teams operating simultaneously at two different sites in the northern half of the valley. Two days of operations focused on convection initiation studies, one day focused on ABL diurnal transition studies, one day focused on internal comparison flights, and the last day of operations focused on cold air drainage flows. The data from these coordinated flights provides insight into the horizontal heterogeneity of the atmospheric state over complex terrain as well as the expected horizontal footprint of RPAS profiles. This dataset, along with others collected by other universities and institutions as a part of the LAPSE-RATE campaign, have been submitted to Zenodo (Greene et al., 2020) for free and open access (DOI:10.5281/zenodo.3737087).

10

## 1 Introduction

Researchers from the University of Oklahoma (OU) joined colleagues from across the world to take part in the Lower Atmospheric Profiling Studies at Elevation – a Remotely-piloted Aircraft Team Experiment (LAPSE-RATE) campaign during 13-19 July 2018 in the San Luis Valley of Colorado. During this campaign, teams from several universities in the United States and Europe partnered with research scientists from government laboratories such as the National Center for Atmospheric Re-

15



search (NCAR), National Severe Storms Laboratory (NSSL) and National Oceanic and Atmospheric Administration (NOAA) to conduct targeted observations of cold air drainage flows, convection initiation, and morning boundary layer transitions with both conventional remote sensors as well as remotely piloted aircraft systems (RPAS, also commonly referred to as uncrewed aircraft systems, UAS). Additionally, the colocation of so many teams provided a unique opportunity to undertake an intensive  
20 comparison of the sensing capabilities of the aerial systems being utilized as a part of the campaign. This manuscript will focus on the data collected by OU in support of the scientific objectives of the campaign, including the platform used, the data acquisition methods, and the processing and archival process. For details regarding OU's contribution to the sensor intercomparison efforts, readers are directed to Barbieri et al. (2019).

Research in RPAS at OU has been ongoing since the 1980s. However, this work entered a new phase in 2009 when re-  
25 searchers in the OU School of Meteorology began exploring ways of utilizing RPAS to take highly resolved profiles of atmospheric state variables (Bonin et al., 2013, 2012), turbulence (Wainwright et al., 2015; Bonin et al., 2015), and ozone (Zielke, 2011) among other phenomena to better understand the evolution and structure of the atmospheric boundary layer (ABL). In 2016, these studies expanded to encompass sensor placement and measurement optimization (Greene et al., 2018), system design and evaluation (Segales et al., 2020a), and sensor integration (Greene et al., 2019) due in large part to the CLOUD-  
30 MAP project which facilitated the development of RPAS for the explicit purpose of conducting atmospheric measurements (Jacob et al., 2018). The capabilities of these weather-sensing RPAS (WxRPAS) have been demonstrated in a variety of collaborative field campaigns (de Boer et al., 2019; Jacob et al., 2018; Koch et al., 2018; Kral et al., 2020, submitted), calibration and validation experiments (Barbieri et al., 2019), and careful comparison against other remote sensing networks (Bell et al., 2020).

OU deployed three CopterSonde 2 quadcopter RPAS as a part of the LAPSE-RATE campaign. This system measures pressure, temperature, humidity, horizontal wind speed, and horizontal wind direction and successfully captured vertical profiles of these variables up to 914 m above ground level (AGL) during this week-long mission. These platforms were deployed to three different sites over the course of the field campaign, typically measuring at two sites simultaneously. This approach resulted in the OU team completing 180 flights that produced quality observational data.

This paper describes the dataset collected by the OU CopterSonde 2 RPAS during LAPSE-RATE. Section 2 will briefly describe the CopterSonde 2 RPAS as well as the operational strategy for this field campaign. Section 3 will highlight some examples of data products available within this dataset, while Section 4 will discuss the data logging, processing, and quality control procedures. Section 5 will outline the format, location, and associated metadata of the publicly available dataset. Finally, Section 6 will provide concluding remarks about the dataset as well as future outlooks regarding the future applications of the  
45 dataset.



**Figure 1.** Photograph of the OU CopterSonde RPAS (Norman, OK, USA) in flight next to an experimental 10 m flux tower.

## 2 Description of the CopterSonde RPAS and Flight Strategy

### 2.1 CopterSonde 2 RPAS

The RPAS utilized for this field campaign was the CopterSonde 2 (Figure 1; see Segales et al., 2020a), which was designed and manufactured by the Center for Autonomous Sensing and Sampling (CASS) at the University of Oklahoma. The CopterSonde 2 is a rotary-wing platform that is based on a modified version of the Lynxmotion HQquad500 wide-X type quadcopter with fixed-pitch rotors that has been optimized for vertical profiling operations. The CopterSonde's technical specifications can be found in Table 1. Additional information regarding the design and development of the CopterSonde series is described in Segales et al. (2020a). The CopterSonde RPAS has been proven to be capable of collecting thermodynamic and kinematic profiles of the atmosphere in a variety of environments from summer in the Southern Great Plains in pre-convective environments (Koch et al., 2018) to polar winter conditions in the Arctic (Kral et al., 2020, submitted). For this deployment, the CopterSonde 2 was piloted under its typical operating parameters except its standard 11" x 5.5" T-style carbon fiber propellers were swapped for a 12" x 5" model to increase the maximum thrust of the vehicle to overcome the higher density altitude in south central Colorado. All the CopterSonde's flights during the campaign were done in a semi-autonomous mode, meaning that the platform flew a



**Table 1.** Technical Specifications of the OU CopterSonde

Frame size	500 mm
All-up weight	2.25 – 2.36 kg
Maximum speed	26.4 m s <sup>-1</sup>
Maximum ascent rate	12.2 m s <sup>-1</sup>
Maximum descent rate	6.5 m s <sup>-1</sup>
Maximum altitude above ground <sup>a</sup>	1800 m
Maximum altitude above sea level	3050 m
Maximum wind speed tolerance	22 m s <sup>-1</sup>
Flight endurance <sup>a</sup>	18.5 min
Operating temperatures <sup>b</sup>	–20 °C – 40 °C
Measured Thermodynamic Variables	Temperature, Pressure, Relative Humidity
Measured Kinematic Variables	Wind Speed, Wind Direction

<sup>a</sup> under favorable weather conditions with low winds.

<sup>b</sup> tested temperatures, the range can be larger than stated.

pre-programmed mission and was only manually controlled by the operator during landing. Commands were sent to the RPAS  
 60 over a telemetry link and data collected were streamed back to the ground station where they were displayed on a customized  
 interface that allowed for real-time monitoring. The ground station and RPAS communicated via a 900 MHz Radio (RFD 900+,  
 RFD Design) that has a range of 40 km.

The CopterSonde 2 is outfitted with sensors that enable it to measure atmospheric state variables as it ascends along its flight  
 path (see Table 4 for details). The wind speed and wind direction were calculated indirectly at 10 Hz using the Wind Vane  
 65 Mode algorithm described in Segales et al. (2020a) which utilizes the roll, pitch, and yaw angles measured with the inertial  
 measurement unit (IMU) on-board the RPAS's autopilot system, the Pixhawk CubeBlack. The pressure was measured at 10 Hz  
 with a MS561 capacitive pressure sensor inside the Pixhawk CubeBlack, which is also utilized for altitude. Atmospheric  
 temperature was measured at 20 Hz with a fast response bead thermistor (International Met Systems). Relative humidity was  
 measured at 10 Hz using the HYT 271 capacitive humidity sensor (Innovative Sensor Technologies). The temperature and  
 70 humidity sensors were enclosed in a custom sensor scoop that was 3D printed out of polylactic acid (PLA). The sensors were  
 located inside the tubular portion of an L-shaped duct and were mounted in an inverted V configuration. At the base of the duct  
 was a smart fan that was programmed to aspirate the sensors at a rate of 12 m s<sup>-1</sup> and was toggled on during ascent at a height  
 of 1.85 m AGL and off during descent at a height of 1.45 m AGL to prevent dust and debris from being pulled into the scoop.  
 Each scoop was distinguished utilizing an identification code and calibrated prior to the field campaign using the procedure  
 75 outlined in Greene et al. (2019). Further information regarding considerations for sensor placement, aspiration, and shielding  
 on the CopterSonde can be found in Greene et al. (2018, 2019). More on the data quality and statistical performances will be  
 discussed in Section 4.

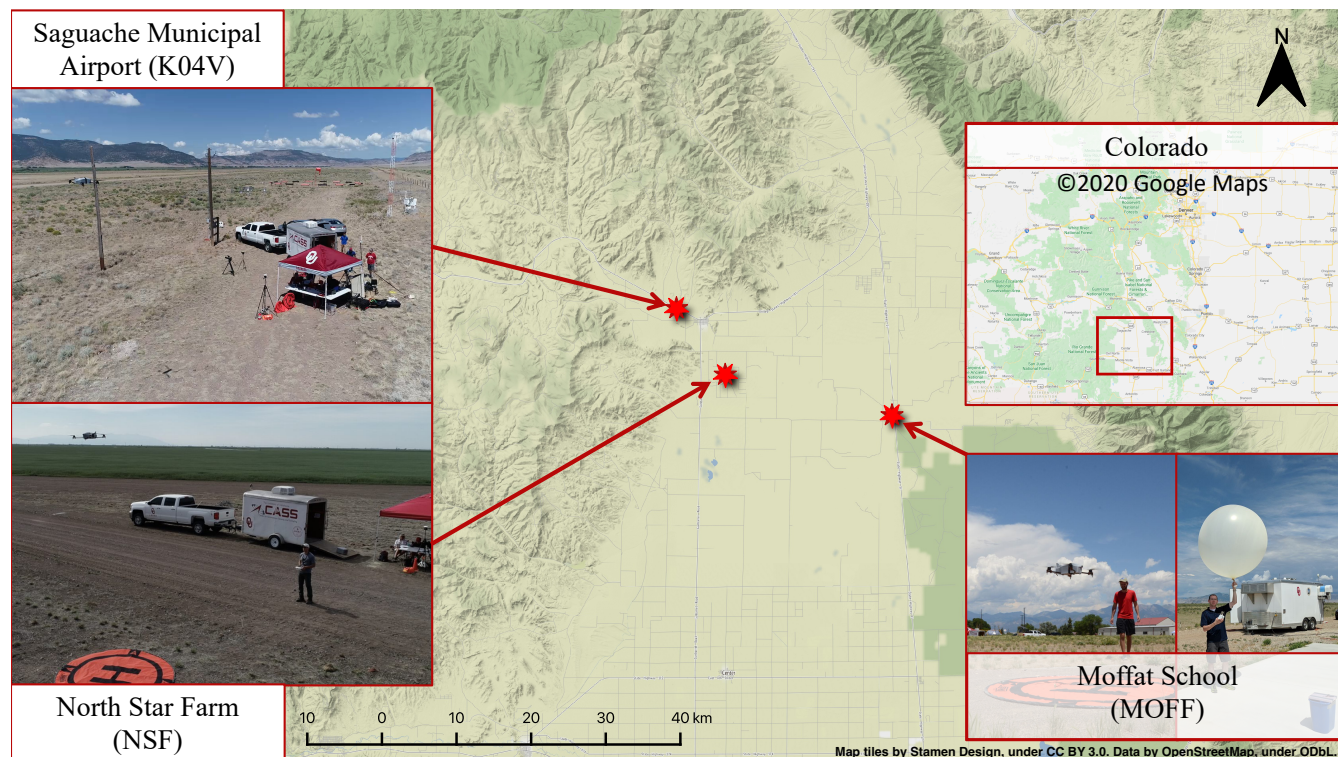


**Figure 2.** Aerial map of the San Luis Valley in south-central Colorado, with CASS deployment locations denoted by the red stars. Inset images beginning from the top left and moving counterclockwise: Saguache Municipal Airport (K04V, photo credit William Doyle), North Star Farm (NSF, photo credit William Doyle), Moffat School (MOFF, photo credit Tyler Bell), and a map of the state of Colorado with the San Luis Valley outlined in red (courtesy Google Maps, ©2020).

## 2.2 Flight Strategies

The LAPSE-RATE campaign featured five unique scientific objectives: morning atmospheric boundary layer transitions, aerosol properties, valley drainage flows, deep convection initiation, and atmospheric turbulence profiling. Each evening, the individual LAPSE-RATE teams would gather for a weather briefing and discuss which objectives would be the most advantageous to target based on forecasts prepared by NCAR scientists. Teams would then distribute themselves across the San Luis Valley to best sample the phenomena of interest. For more detailed information about the overall campaign goals, science objectives, synoptic and mesoscale conditions driving the selection of objectives, please see the LAPSE-RATE overview article in this special issue (de Boer et al., 2020).

The CopterSonde was deployed at three different locations across the San Luis Valley in support of LAPSE-RATE scientific objectives. These locations were Moffat Consolidated School (MOFF), Saguache Municipal Airport (K04V), and the southern edge of North Star Farms (NSF). Latitude and longitudes of these deployment locations as well as their altitude above mean sea level (m MSL) are summarized in Table 2. A visual representation of these locations with respect to the layout of the valley



**Table 2.** List of sites during LAPSE-RATE where CASS operated.

Site (Abbreviation)	Latitude (°N)	Longitude (°E)	Altitude (m MSL)
Saguache Municipal Airfield (K04V)	38.099156	-106.171331	2385.2
Moffat School (MOFF)	37.997587	-105.911795	2305.6
North Star Farm (NSF)	38.036093	-106.112658	2330.8

90 is provided in Figure 2, with the inset focusing on the layout of the multiple assets operating at MOFF. The MOFF and NSF sites were both located in the central portion of the valley whereas K04V was situated in a narrowing section of the valley with steeper valley walls to the northwest of NSF. MOFF and K04V were dominated by scrublands while NSF was primarily comprised of irrigated cropland.

OU deployed a team daily to MOFF regardless of objective due to the collocation of the Collaborative Lower Atmosphere  
95 Mobile Profiling Station (CLAMPS) at the site. Not only did this create a local supersite in the central region of the valley, it facilitated the intercomparison of the RPAS with more conventional instrumentation such as radiosondes, atmospheric emitted radiance interferometer (AERI), microwave radiometer (MWR), and Doppler LIDAR (Bell et al., 2020; Wagner et al., 2019). A second OU team was deployed to one of three locations depending on the daily objective. For the convection initiation (CI) and boundary layer transition (BLT) study days, the second team set up at K04V. For the cold air drainage study, the team  
100 deployed to NSF. Across all three sites, 180 successful flights were completed in support of LAPSE-RATE. Details regarding the number of flights per day, daily science objectives, start and stop times, and specific vehicles used are summarized in Table 3.

All flights completed by OU as a part of LAPSE-RATE were conducted either under Federal Aviation Authority (FAA) Part 107 regulations or under the Oklahoma State University's FAA Certificate of Authority (COA) 2018-WSA-1542 effective from  
105 13 - 22 July 2018. This COA permitted daytime operations of small RPAS weighting less than 25 kg (55 lbs.) at speeds less than  $45 \text{ m s}^{-1}$  (87 kts) in Class E and G airspace below 914 m AGL and not exceeding 3,657 m above mean sea level (MSL) in the vicinity of Alamosa County, CO under the jurisdiction of the Denver Air Route Traffic Control Center (ARTCC). Typical COA provisions for airworthiness, operations, safety protocols, Notice to Airmen (NOTAMs), reporting, and registration were applied; however, special provisions were necessary for the coordination and deconfliction of the myriad of teams participat-  
110 ing in flight operations as part of LAPSE-RATE. Instead of requiring each individual team to submit NOTAMs, discussions between LAPSE-RATE participants, the FAA, and Denver ARTCC lead to the definition of a common area of operations that could cover the entirety of the planned LAPSE-RATE observations. Additional deconfliction was also necessary with nearby airports, Military Training Routes (MTRs), or other restricted airspaces such as the Great Sand Dunes National Park. Within this area, two NOTAM subareas were defined so that the most appropriate areas could be activated with the necessary 24-hr  
115 notice based on the next day's scientific objectives. Emergency procedures for lost links, radio communications, and other potential anomalies also had special provisions due to the number of teams operating in proximity to each other. In addition



**Table 3.** Summary of flights for each day broken down by aircraft and location. Local time during the campaign was Mountain Daylight Time (UTC−6).

Date	Time Start	Time Stop	Science Objective	Site 1	Aircraft Number	Flight Count	Site 2	Aircraft Number	Flight Count	Daily Total
14 July 2018	1430 UTC	2130 UTC	CASS Tests	MOFF	OU944	4	–	–	–	4
15 July 2018	1330 UTC	1945 UTC	CI	MOFF	OU944 OU955	2 18	K04V	OU946	14	34
16 July 2018	1330 UTC	2115 UTC	CI	MOFF	OU955	26	K04V	OU946	21	47
17 July 2018	1330 UTC	2130 UTC	CASS Tests	MOFF	OU944	5	MOFF	OU946	9	14
18 July 2018	1230 UTC	1945 UTC	ABL Transition	MOFF	OU944	14	K04V	OU946	21	35
19 July 2018	1115 UTC	1700 UTC	Drainage	MOFF	OU944	24	NSF	OU946	22	46
<b>MOFF Total</b>						<b>93</b>	<b>K04V &amp; NSF Total</b>		<b>87</b>	<b>180</b>

to the COA provisions, each OU operations area was overseen by a licensed private pilot who assisted with overseeing the airspace and deconflicting RPAS operations from general aviation traffic.

CopterSonde missions were programmed to fly a vertical ascent from the surface to 914 m AGL, utilizing the platforms wind vane mode to continuously orient itself into the wind. This permitted the RPAS to sample the vertical structure of pressure, temperature, humidity, wind speed, and wind direction in a controlled and repeatable manner that minimized influences from the platform itself (Segales et al., 2020a). These flights will be referred to as profiles in subsequent text and tables. These profiles consisted of an automatic takeoff, vertical ascent at a rate of  $3.5 \text{ m s}^{-1}$ , loiter for 10 s at the apex of the ascent, and controlled decent to 10 m at a rate of  $6 \text{ m s}^{-1}$ . Once the platform completed its decent, it would be brought in for a landing manually.

Profiles were conducted on a 15- or 30-min cadence depending on the day’s primary scientific objective and how rapidly the thermodynamic and kinematic parameters of the ABL were evolving. As the CopterSonde was collocated with CLAMPS at MOFF, RPAS profiles would often coincide with radiosonde launches. When this would occur, the RPAS launch would be held until the balloon cleared the airspace (about 60 s), and then would proceed as normal.

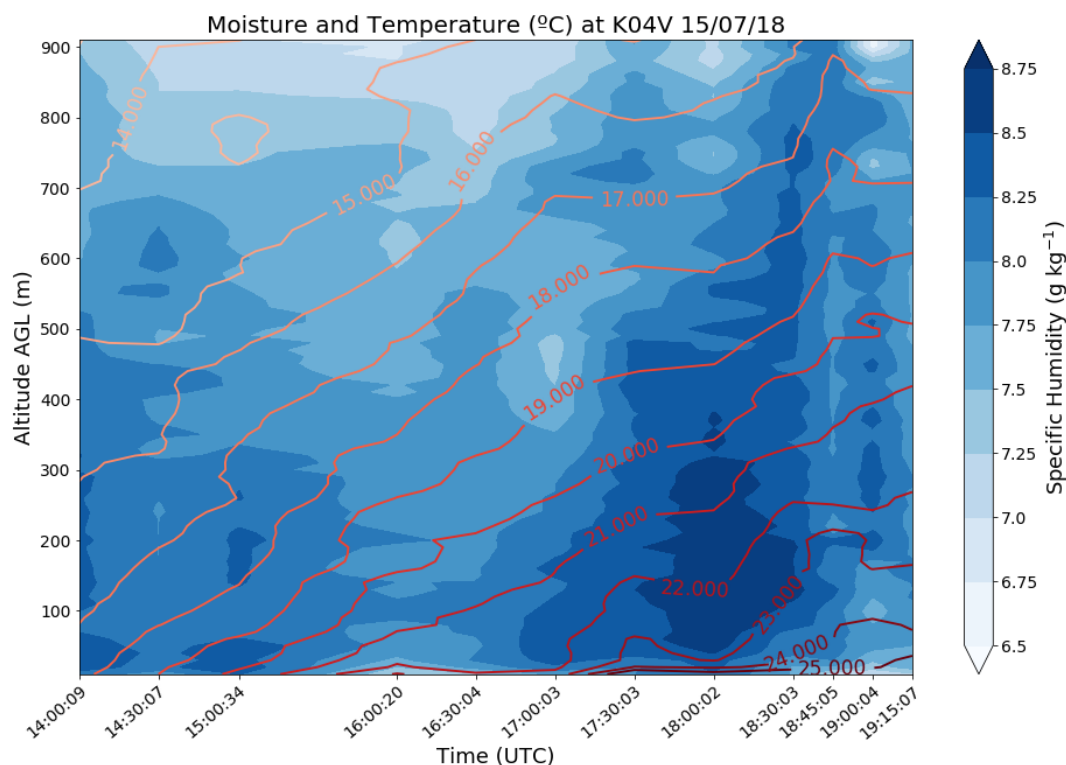


**Figure 3.** Time-height cross-section view of moisture and temperature measurements at K04V on 15 July 2018. This day experienced deep convection. Shaded field is specific humidity ( $\text{g kg}^{-1}$ ). Contours are temperature ( $^{\circ}\text{C}$ ). Values are interpolated through time at each level between successive flights.

### 130 3 Examples of Flight Data

#### 3.1 Convective Initiation – 15 July 2018

The environment on the morning of 15 July 2018 was rich in moisture with decreasing stability as the day progressed. This made for good conditions to target pre-convective measurements. The low wind shear and weak synoptic flow were conducive for isolated CI. This aided in spatially discerning precursors to CI. Two CASS teams were stationed at MOFF and K04V, approximately 18 km apart, with aircraft OU946 and OU955, respectively. Both teams began flying at 1400 UTC (0900 MDT).  
135 The team at MOFF had profiles every 15 minutes until 1945 UTC (1445 MDT). The team at K04V had profiles nearly every 30 minutes until 1915 UTC (1415 MDT). The maximum flight height for both teams was 914 m. Figures 3 and 4 show differences in how moisture and temperature evolve with time at each site. Figure 3 shows specific humidity increasing at K04V with time, meanwhile decreasing at MOFF (Figure 4). Evaporation of additional moisture over MOFF slowed daytime heating. Although  
140 both sites had similar temperature fields, Figure 3 shows the temperature increasing faster with time. Since K04V was slightly drier, this led to faster destabilization and possibly preferential CI. Figure 3 also shows the post convection cool down around

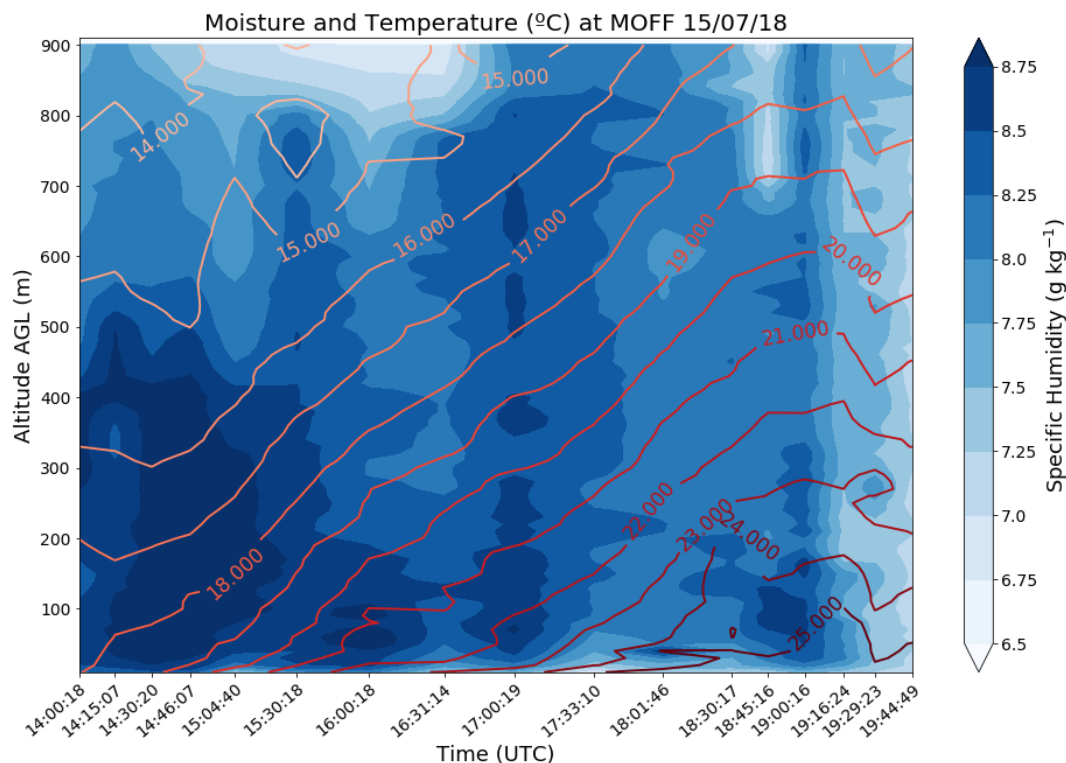


**Figure 4.** Time-height cross-section view of moisture and temperature measurements at MOFF on 15 July 2018. This day experienced deep convection. Shaded field is specific humidity ( $\text{g kg}^{-1}$ ). Contours are temperature ( $^{\circ}\text{C}$ ). Values are interpolated through time at each level between successive flights.

1800 UTC. Even though the sites were not very far apart, there is a difference in the evolution of specific humidity. More cases would need to be analyzed to determine if this could have implicated the location of CI.

### 3.2 CASS Test Flights – 17 July 2018

145 The LAPSE-RATE participants collectively decided for 17 July 2018 to be utilized for individual group research objectives, and so both mobile CASS teams decided to combine at the MOFF site for intercomparison flights between the CopterSondes and against CLAMPS. Between OU944 and OU946, 14 total vertical profile flights were conducted throughout the afternoon, 8 of which were simultaneous for direct comparisons across platforms (Table 3). Several of these flights were also accompanied by radiosonde launches directly before the vertical profiles, which were included along with the CLAMPS AERI and Doppler  
150 LIDAR observations in the comparison study by Bell et al. (2020). During these flights, the pair of CopterSondes flew about 10–20 m apart horizontally, and were also displaced about 50 m from the radiosonde launch site. An example of a direct comparison between OU944 and OU946 on the afternoon of 17 July (Figure 5) shows that both aircraft observed similar thermodynamic features with a well-mixed, dry adiabatic atmosphere up to around 600 m AGL, above which is notably drier

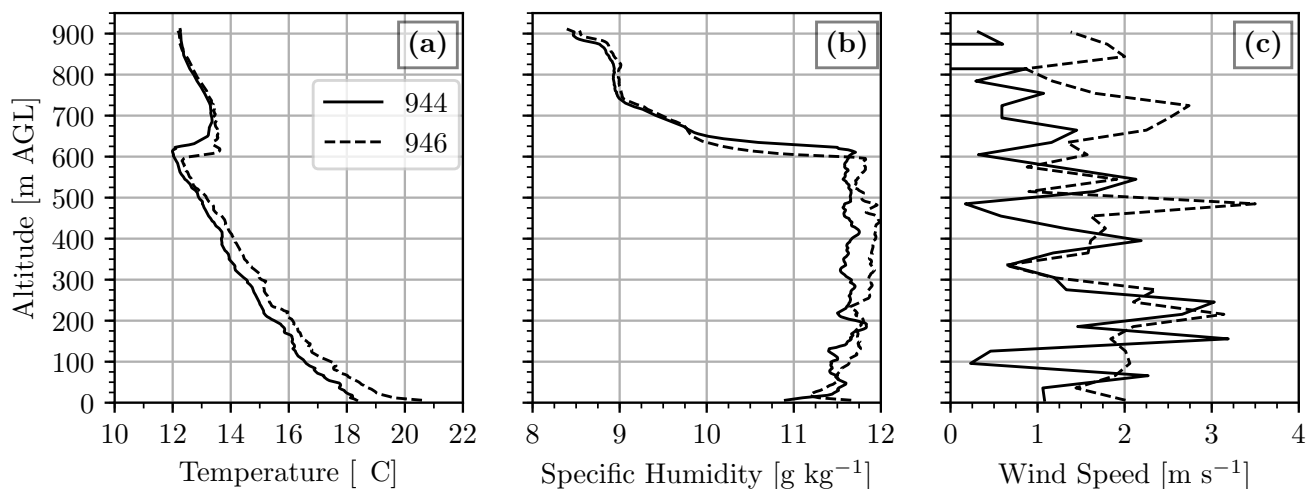


**Figure 5.** Comparisons of two CopterSonde flights launched simultaneously at 16:02:55 UTC at MOFF on 17 July 2018. In all panels, the solid and dashed black lines represent the OU944 and OU946 aircraft, respectively. Shown here are (a) temperature ( $^{\circ}\text{C}$ ), (b) specific humidity ( $\text{g kg}^{-1}$ ), and (c) horizontal wind speed ( $\text{m s}^{-1}$ ) versus altitude above ground level (AGL). Note that all data are included in (a) and (b), but data are subsampled at every eight points in (c) for clarity. Wind speed and direction in general throughout the campaign were considerably variable in time and space.

and warmer than the ABL below. While a small bias between the two aircraft exists in temperature and specific humidity, the profile shapes and inversion magnitudes are consistent across the platforms. Furthermore, winds throughout the depth of the atmosphere were weak and variable, but still show reasonable agreement between the two aircraft. For a more detailed perspective on the relative accuracy and precision of this dataset, readers are again referred to Barbieri et al. (2019) and Bell et al. (2020).

### 3.3 Boundary Layer Transition – 18 July 2018

The morning of 18 July 2018, featured weak ambient synoptic-scale weather conditions and clear skies throughout the valley that enabled targeted measurements of the diurnal ABL transition. On this day, the two CASS teams were situated at the MOFF and K04V sites, with operations taking place from 1230–1945 UTC (0630–1345 MDT; Table 3). At both locations, vertical profiles to 914 m AGL were flown once every 15 min for the majority of the day. This particular case exemplified a canonical morning ABL transition, marked by a surface-based temperature inversion with a residual layer apparent atop beginning around 300 m at local sunrise (Figure 6). After the sun rose above the Rocky Mountains and flooded the valley with shortwave radiation, vertical mixing dominated the lowest levels of the ABL. A surface-based dry adiabatic layer became present around 1415 UTC (Figure 6) as the ABL grew in depth. Surface-based vertical mixing appears to dominate the surface layer for several hours this morning, as the atmosphere above 300 m remains relatively steady-state for most of the early growth

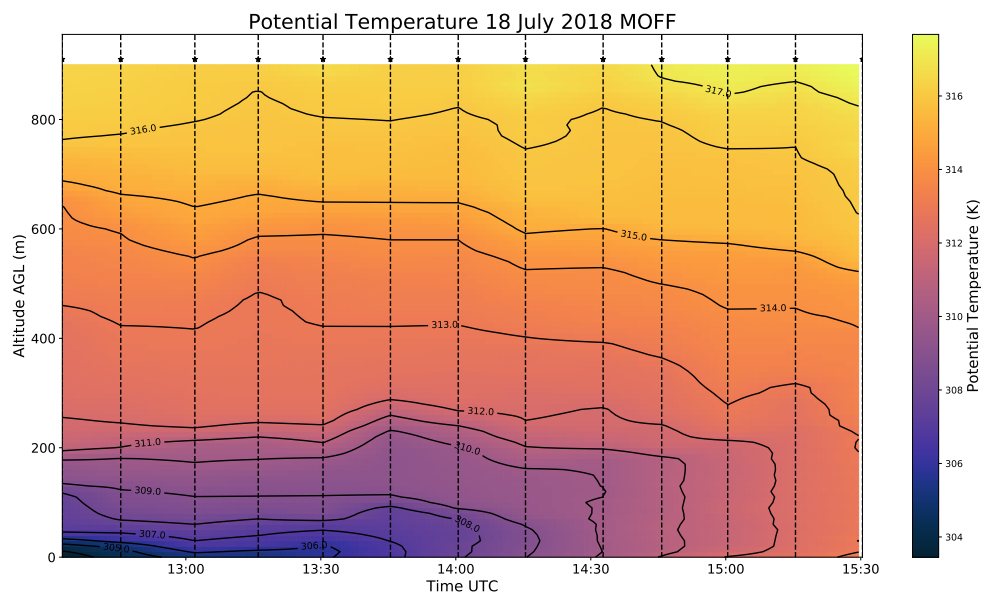


**Figure 6.** Time-height cross-section view of CopterSonde potential temperature observations at the MOFF on 18 July 2018. Shaded and contoured are potential temperature (K), and vertical dashed lines represent the time of CopterSonde flights. The star markers represent the maximum altitude achieved for a given profile. Values are interpolated through time at each level between successive flights.

of the convective boundary layer. Entrainment-based heating of the growing ABL is also apparent by tracking the level of the strongest vertical potential temperature gradient through the morning (Figure 6).  
170

### 3.4 Drainage Flow – 19 July 2018

The morning of 19 July 2018, was characterized by relatively quiescent conditions, making it the target of katabatic drainage flow observations. CASS flew CopterSondes from two locations (MOFF and NSF), conducting 46 total vertical profiles at 15 min intervals between 1115–1700 UTC (Table 3). A cursory glance at potential temperature in time-height coordinates from this day at the NSF site (Figure 7) reveals a similar ABL transition as observed on the previous day from the MOFF site (Figure 6). However, closer inspection reveals several harmonic structures, with a relative warm anomaly around 100 m AGL with a period of roughly 15 min at 1315 UTC propagating vertically through the next 4–5 profiles. Due to the highly stratified nature of the atmosphere at this time and the presence of complex topography, it is possible these disturbances are the result of internal gravity waves. Further investigation is necessary to elucidate specific details on this phenomenon and its sensitivity to  
175  
180 spatial and temporal interpolation schemes.

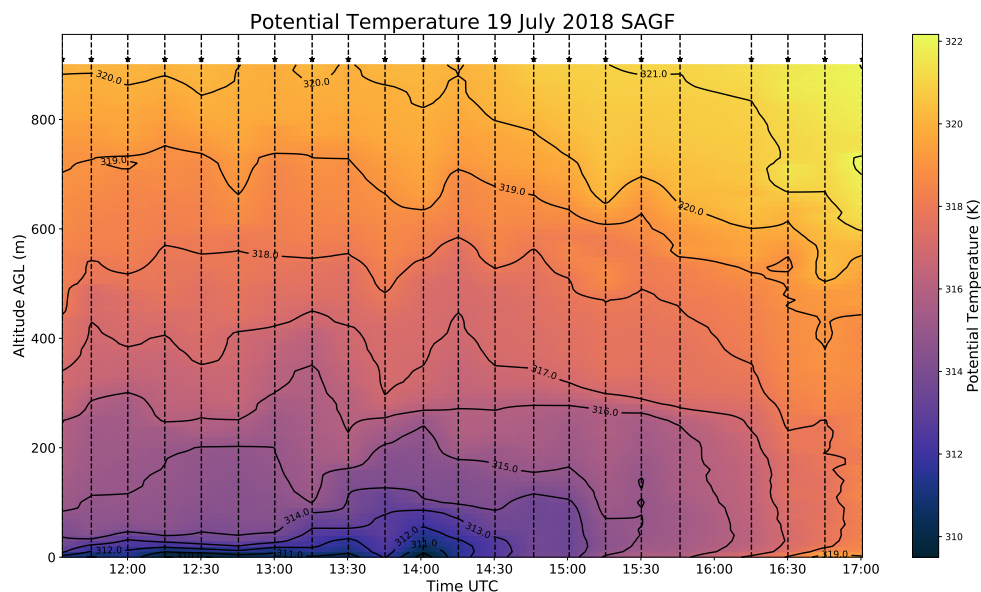


**Figure 7.** Time-height cross-section view of CopterSonde potential temperature observations at the Saguache farm location on 19 July 2018. Figure notations follow the same conventions as in Figure 6.

#### 4 Data processing

The data collected by the CopterSondes were processed and quality controlled by CASS after the conclusion of the LAPSE-RATE campaign. The CopterSondes' Pixhawk autopilot system output and store a binary file on an on-board SD card during each flight, which includes logs of the aircraft's attitude angles, GPS positions, accelerations, and readings from the 3 temperature and 3 relative humidity sensors. In this format, the data are equivalent to the United States Department of Energy (DoE) Atmospheric Radiation Measurement (ARM) program's data archive "a0" level. Because the sensors log at different rates to the SD card, the binary files were converted to JavaScript Object Notation (JSON) format and relevant data parameters were interpolated/downsampled to a common 10 Hz time vector in comma-separated values (CSV) format (a1 level). More information about how the CopterSonde fuses sensor readings with autopilot features can be found in Segales et al. (2020a), and the autopilot code is freely available at Segales et al. (2020b).

After converting the raw binary flight log files to csv format, offsets for each temperature and relative humidity sensor were applied. These offsets were determined in the manner described by Greene et al. (2019) and Segales et al. (2020a), which involved isolating the CopterSondes' front L-duct sensor payloads in an environmentally-controlled chamber operated by the Oklahoma Mesonet with National Institutes of Standards and Technology (NIST) traceable sensors as references. Furthermore, at this stage, the CopterSonde attitude angles were averaged to estimate the horizontal wind speed and direction using linear regression coefficients determined by hovering next to Oklahoma Mesonet towers as a reference. This process is outlined in Greene (2018) and Segales et al. (2020a) (based on Neumann and Bartholmai, 2015; Palomaki et al., 2017).



Once the thermodynamic and kinematic calibrations were accounted for, the post-processing algorithm objectively determined the window of time for evaluation. This was chosen to be between 6 m AGL and the maximum point of the direct vertical profile (typically 914 m AGL during LAPSE-RATE) on the *ascending* portion only, averaged to 3-m bins as estimated by the Pixhawk autopilot's barometer and GPS sensors (Segales et al., 2020a). These criteria were chosen for several reasons, primarily to do with the relationships between ascent rate and sensor response time. Data averaging began at 6 m so as to avoid any possible contamination due to propeller wash interacting with the ground. The ascent portion is chosen because the flight patterns of the CopterSonde were chosen to maximize the achievable flight altitude and involves descending much more rapidly than ascending. Therefore, the descent portion suffers more from thermodynamic sensor response time issues. Furthermore, the physics behind the method of estimating horizontal wind speeds are not the same given the body forcings on a descending rotary-wing RPAS. Finally, the 3 m averaging interval was chosen as a combination of ascending at  $3 \text{ m s}^{-1}$  and an approximate time constant of the sensor payload of 1 s.

In this window of time for analysis, time-series data from each of the temperature and relative humidity sensors were plotted and relative outlier sensors were subjectively omitted from further processing if they did not qualitatively or quantitatively follow the trends of the other sensors. All remaining sensor data were averaged together to yield a single measurement of temperature and relative humidity at each 3-m altitude interval. These post-processed ascent profiles were then exported in netCDF format (b1 level) that contain self-describing metadata including e.g., the specific aircraft and flight description. These file contents are described in Table 4. The reader is directed to Barbieri et al. (2019) and Bell et al. (2020) for more information on measurement accuracy, and Greene et al. (2018, 2019) for more regarding considerations taken for temperature sensor placement on-board the CopterSonde.

## 5 Data availability

The OU CopterSonde data files from the LAPSE-RATE campaign are available for public access from the Zenodo data repository (Greene et al., 2020). They are in netCDF format with self-describing metadata and are organized by flight, aircraft tail number, and location. Included in each file are quality-controlled thermodynamic (temperature, pressure, humidity) and kinematic (wind speed and direction) measurements from collected by CASS during the LAPSE-RATE campaign from 14–19 July 2018. These files are from the fleet of 3 individual CopterSonde rotary-wing RPAS used during the campaign.

The files follow a naming convention of UOK.ppppp.lv.yyyymmdd.hhmmss.cdf, where ppppp is a platform identification code (one of “OU944”, “OU946”, “OU955”), lv is the data file processing level, and yyyymmdd.hhmmss is the year-month-date.hour-minute-second of the file start date and time. Further information is included in the readme text file in this repository.

## 6 Summary

During July 2018, researchers from OU's CASS participated alongside federal and university partners in the LAPSE-RATE field campaign in San Luis Valley, Colorado, USA. The OU team successfully completed 180 flights using three RPAS over



**Table 4.** Description of the thermodynamic and kinematic parameters available in each CopterSonde data file. Also includes information on the method each parameter was measured along with their relative accuracies based on Bell et al. (2020) compared to Vaisala RS92-SGP radiosondes.

Parameter	Method	Accuracy
Temperature	3 iMet-XF Bead Thermistors	$\pm 0.5^{\circ}\text{C}$
Relative Humidity	3 IST HYT-271 Capacative Hygrometers Converted to dewpoint temperature then recalculated using fast-response iMet-XF bead thermistors	$\pm 2\%$
Dewpoint Temperature	Converted from temperature and relative humidity measured by the 3 IST HYT-271 sensors	$\pm 0.5^{\circ}\text{C}$
Pressure	TE MS5611 Barometric Pressure Sensor (inside Pixhawk 2.1 Autopilot)	$\pm 1.5\text{ hPa}$
Wind Speed	Linear regression of tilt angles compared to reference	$\pm 0.6\text{ m s}^{-1}$
Wind Direction	Linear regression of tilt angles compared to reference	$\pm 4^{\circ}$

the course of six days of operation to collect vertical profiles of the thermodynamic and kinematic state of the ABL. This article describes sampling strategies, data collection, platform intercomparability, data quality and processing, and the dataset's possible applications to convective initiation, drainage flows, and ABL transitions.

The data available from these flights provides measurements of temperature, humidity, pressure, wind speed, and wind direction at a higher spatiotemporal resolution in the ABL than many conventional strategies, such as radiosondes, which will significantly contribute to characterizing the ABL within the San Luis Valley during the campaign. The data collected from the operations and platforms described here are uploaded and available for download through the Zenodo data repository (DOI:10.5281/zenodo.3737087).



*Author contributions.* Field Campaign Planning: E.P.L and P.C.; Data Collection: E.P.L, B.G., T.B., A.S., G.A., W.D, S.K., D.T., and P.C.; Data processing and quality control: B.G.; Data Analysis and Visualization: B.G., F.L., and T.B.; Writing: E.P.L, B.G., and F.L.; Supervision: P.C. and E.P.L; Funding acquisition: P.C.

240 *Competing interests.* The authors declare that they have no conflicts of interest.

*Acknowledgements.* This research has been supported in part by the National Science Foundation under Grant No. 1539070 and internal funding from the University of Oklahoma Office of the Vice President for Research and Partnerships. The authors would also like to thank the Moffat Consolidated School for the use of their parking lot and facilities for the duration of the campaign as well as the greater San Luis Valley community for welcoming the LAPSE-RATE campaign and providing land access for flight operations. Additional support for field  
245 operations in Colorado were provided by University of Oklahoma undergraduate research assistants Brandon Albert, Samantha Bashcky, Christopher Hughes, Mark Thiel, and Brent Wolf.



## References

- Barbieri, L., Kral, S. T., Bailey, S. C., Frazier, A. E., Jacob, J. D., Reuder, J., Brus, D., Chilson, P. B., Crick, C., Detweiler, C., et al.: Intercomparison of small unmanned aircraft system (sUAS) measurements for atmospheric science during the LAPSE-RATE campaign, *Sensors*, 19, 2179, 2019.
- 250 Bell, T. M., Greene, B. R., Klein, P. M., Carney, M., and Chilson, P. B.: Confronting the boundary layer data gap: evaluating new and existing methodologies of probing the lower atmosphere, *Atmospheric Measurement Techniques*, 13, 3855–3872, <https://doi.org/10.5194/amt-13-3855-2020>, <https://amt.copernicus.org/articles/13/3855/2020/>, 2020.
- Bonin, T., Chilson, P., Zielke, B., and Fedorovich, E.: Observations of the Early Evening Boundary-Layer Transition Using a Small Unmanned Aerial System, *Boundary-Layer Meteorology*, 146, 119–132, <https://doi.org/10.1007/s10546-012-9760-3>, <http://dx.doi.org/10.1007/s10546-012-9760-3>, 2012.
- 255 Bonin, T., Chilson, P., Zielke, B., Klein, P., and Leeman, J.: Comparison and application of wind retrieval algorithms for small unmanned aerial systems, *Geoscientific Instrumentation, Methods and Data Systems*, 2, 177–187, 2013.
- Bonin, T. A., Blumberg, W. G., Klein, P. M., and Chilson, P. B.: Thermodynamic and turbulence characteristics of the southern great plains nocturnal boundary layer under differing turbulent regimes, *Bound.-Lay. Meteorol.*, 157, 401–420, <https://doi.org/10.1007/s10546-015-0072-2>, 2015.
- 260 de Boer, G., Argrow, B., Cassano, J., Cione, J., Frew, E., Lawrence, D., Wick, G., and Wolff, C.: Advancing Unmanned Aerial Capabilities for Atmospheric Research, *Bulletin of the American Meteorological Society*, 100, ES105–ES108, <https://doi.org/10.1175/BAMS-D-18-0254.1>, 2019.
- 265 de Boer, G., Houston, A., Jacob, J., Chilson, P. B., Smith, S. W., Argrow, B., Lawrence, D., Elston, J., Brus, D., Kemppinen, O., Klein, P., Lundquist, J. K., Waugh, S., Bailey, S. C. C., Frazier, A., Sama, M. P., Crick, C., Schmale III, D., Pinto, J., Pillar-Little, E. A., Natalie, V., and Jensen, A.: Data Generated During the 2018 LAPSE-RATE Campaign: An Introduction and Overview, *Earth System Science Data Discussions*, 2020, 1–15, <https://doi.org/10.5194/essd-2020-98>, <https://essd.copernicus.org/preprints/essd-2020-98/>, 2020.
- Greene, B. R.: Boundary Layer Profiling Using Rotary-Wing Unmanned Aircraft Systems: Filling the Atmospheric Data Gap, Master's thesis, The University of Oklahoma, <https://hdl.handle.net/11244/301374>, 2018.
- 270 Greene, B. R., Segales, A. R., Waugh, S., Duthoit, S., and Chilson, P. B.: Considerations for temperature sensor placement on rotary-wing unmanned aircraft systems, *Atmospheric Measurement Techniques*, 11, 5519–5530, <https://doi.org/10.5194/amt-11-5519-2018>, <https://www.atmos-meas-tech.net/11/5519/2018/>, 2018.
- Greene, B. R., Segales, A. R., Bell, T. M., Pillar-Little, E. A., and Chilson, P. B.: Environmental and sensor integration influences on temperature measurements by rotary-wing unmanned aircraft systems, *Sensors*, 19, 1470, 2019.
- 275 Greene, B. R., Bell, T. M., Pillar-Little, E. A., Segales, A. R., Britto Hupsel de Azevedo, G., Doyle, W., Tripp, D. D., Kanneganti, S. T., and Chilson, P. B.: University of Oklahoma CopterSonde Files from LAPSE-RATE, <https://doi.org/10.5281/zenodo.3737087>, <https://doi.org/10.5281/zenodo.3737087>, 2020.
- Jacob, J., Chilson, P., Houston, A., and Smith, S.: Considerations for atmospheric measurements with small unmanned Aircraft systems, *Atmosphere*, 9, 252, 2018.
- 280 Koch, S. E., Fengler, M., Chilson, P. B., Elmore, K. L., Argrow, B., Andra, D. L., and Lindley, T.: On the Use of Unmanned Aircraft for Sampling Mesoscale Phenomena in the Preconvective Boundary Layer, *Journal of Atmospheric and Oceanic Technology*, 35, 2265–2288, <https://doi.org/10.1175/JTECH-D-18-0101.1>, 2018.



- 285 Kral, S., Reuder, J., Seidl, A., Båserud, L., Flacké Haualand, K., Vihma, T., Suomi, I., Urbancic, G., Kouznetsov, R., Lorenz, T., Mayer, S.,  
Steenefeld, G.-J., Holtslag, A., Greene, B., Chilson, P., Pillar-Little, E., and Wrenger, B.: The Innovative Strategies for Observations in  
the Arctic Atmospheric Boundary Layer Project (ISOBAR), *Bull. Amer. Meteor. Soc.*, 2020, submitted.
- Neumann, P. P. and Bartholmai, M.: Real-time wind estimation on a micro unmanned aerial vehicle using its inertial measurement unit,  
*Sensor Actuat. A-Phys.*, 235, 300–310, <https://doi.org/10.1016/j.sna.2015.09.036>, 2015.
- Palomaki, R. T., Rose, N. T., van den Bossche, M., Sherman, T. J., and De Wekker, S. F.: Wind estimation in the lower atmosphere using  
290 multicopter aircraft, *J. Atmos. Ocean. Tech.*, 34, 1183–1191, <https://doi.org/10.1175/JTECH-D-16-0177.1>, 2017.
- Segales, A. R., Greene, B. R., Bell, T. M., Doyle, W., Martin, J. J., Pillar-Little, E. A., and Chilson, P. B.: The CopterSonde: an insight into  
the development of a smart unmanned aircraft system for atmospheric boundary layer research, *Atmospheric Measurement Techniques*,  
13, 2833–2848, <https://doi.org/10.5194/amt-13-2833-2020>, <https://www.atmos-meas-tech.net/13/2833/2020/>, 2020a.
- Segales, A. R., Tridgell, A., Mackay, R., Barker, P., Marchi, L. D., WickedShell, Riseborough, P., Pittenger, T., jason4short, Kancir, P.,  
295 jschall, Hall, L., de Sousa, G. J., Osborne, M., Walser, J., Hickey, P., Lucas, A., Lefebvre, R., Purohit, S. B., Ferreira, F., murata, k.,  
de Oliveira Filho, C. M., Staroselskii, G., Morphett, G., Denecke, M., Whitehorn, M., Hall, P., Shamaev, E., Jehangir, R., Goppert,  
J., and Vilches, V. M.: oucass/CASS-ardupilot: CASSv1.6.0-Copter-3.6.12, <https://doi.org/10.5281/zenodo.3494655>, <https://doi.org/10.5281/zenodo.3494655>, 2020b.
- Wagner, T. J., Klein, P. M., and Turner, D. D.: A New Generation of Ground-Based Mobile Platforms for Active and Passive Profiling of the  
300 Boundary Layer, *Bulletin of the American Meteorological Society*, 100, 137–153, <https://doi.org/10.1175/BAMS-D-17-0165.1>, 2019.
- Wainwright, C. E., Bonin, T. A., Chilson, P. B., Gibbs, J. A., Fedorovich, E., and Palmer, R. D.: Methods for evaluating the temperature  
structure-function parameter using unmanned aerial systems and large-eddy simulation, *Boundary-Layer Meteorology*, 155, 189–208,  
2015.
- Zielke, B.: A Procedure for Obtaining High-Density In-Situ Measurements of Ozone Concentration Within the Planetary Boundary Layer,  
305 Master's thesis, University of Oklahoma, 2011.